CryoSat-2 Precise Orbit Determination and Indirect Calibration of SIRAL

End of Commissioning Phase Report

E. Schrama, M. Naeije, Y. Yi, P. Visser, and C. Shum

Delft Institute for Earth-Oriented Space Research
Delft University of Technology
Kluyverweg 1, 2629 HS Delft
The Netherlands

This document was typeset with LaTeX 2$_\varepsilon$.
The layout was designed by Remko Scharroo

Contents

Chapter *1*

Introduction

In this report DEOS/A&S will report on the status of their activities at the end of the commissioning phase of the Cryosat-2 mission which was successfully launched on 8-april-2010. The work packages on which we report in this document are WP310 which concerns Precision Orbit Determination (POD) and work packages WP520 and WP530 which are both related to the SIRAL altimeter in LRM as explained in *Schrama et al.* [2009].

Chapter *2*

WP 310: Precise Orbit Determination (POD)

This chapter describes status of precision orbit determination activities after completion of the commissioning phase as described in contract *Schrama et al.* [2009]. Within the framework of this contract we will compute trajectories of the Cryosat-2 satellite which are determined from DORIS and Satellite Laser Ranging (SLR) data for which the GEODYN-2 software is used, cf. *Pavlis DE* [2006]. In section 2.1 we discuss the a summary of the assumed models, reference data and observation datasets used for this study. In section 2.2 we report on the Cryosat-2 POD results obtained with the GEODYN-2 software. In section 2.3 we show the comparison to DORIS navigator orbit, Centre Nationales de Etudes Spatialles (CNES) MOE and POE trajectories. In section 2.4 we present our conclusions and recommendation of this study.

2.1 Introduction

The section of astrodynamics and space missions within the faculty of aerospace engineering at the Delft University of technology, short DEOS/A&S , worked on the validation of Cryosat-2 orbits which are determined by DORIS and SLR.

Precision orbit determination at DEOS/A&S for Cryosat-2 is performed with the help of the GEODYN-2 software developed by the space geodesy group at the Goddard Space Flight Center in Greenbelt Maryland. The provided tools are extended with additional capabilities for processing new data types such as PRARE data and altimeter crossover data. Furthermore DEOS/A&S developed new tools to streamline DORIS satellite tracking data and also updating for instance earth orientation parameter (EOP) tables, magnetic field data, solar flux data and a variety of geophysical models.

The remainder of this section discusses the POD infrastructure in 2.1.1. The implementation of the ground station coordinates is described in section 2.1.2, the attitude model of Cryosat-2 is discussed in section 2.1.3, the solar radiation pressure (SRP) model of the satellite is in section 2.1.4 and the antenna offsets are discussed in sub-section 2.1.5, a description of the satellite mass and center of gravity is in section 2.1.6.

2.1.1 POD infrastructure

The precision orbit determination infrastructure for Cryosat-2 is as follows:

- A front-end linux server with the functionality to retrieve 10s integrated DORIS Doppler and SLR information related to Cryosat-2 from public internet sources. The main International Doris Service (IDS) repository for DORIS data is **ftp://doris.ensg.ign.fr/pub/doris**, a backup IDS repository is **ftp://cddis.gsfc.nasa.gov/pub/doris**. The main source for retrieving satellite laser ranging data is the Crustal Dynamics Data Information System (CDDIS) accessible via **ftp://cddis.gsfc.nasa.gov/pub/slr**, and a backup SLR data source at the Eurolas Data Center (EDC) accessible via **ftp://ftp.dgfi.badw-muenchen.de/pub/slr**.
- A front-end linux server with the functionality to retrieve medium orbit ephemeris (MOE) files, precision orbit ephemeris files (POE) files, satellite maneuver and mass data, quaternion data, DIODE navigator orbits, and receiver carrier phase data from ESA repositories dedicated to the Cryosat-2 commissioning phase. MOE and POE orbit data arrives via ftp to **cryo-tudelft@calval-pds.cryosat.esa.int**, DIODE Navigator and receiver carrier phase data is retrieved by means of ftp to **cryo-tudelft@calval-pds.cryosat.esa.int**. Spacecraft mass and maneuver events are received via sftp to **cryo-tud@cryxsera.esoc.ops.esa.int**, and star tracker data arrives via FTP to **cryo-str@calval-pds.cryosat.esa.int**
- A client linux workstation to receive the two line element (TLE) sets acquired by North American Aerospace Defense Command (NORAD). This provides a backup mechanism for initializing the initial state vector for a new arc (i.e. a defined time window within which a trajectory will be reconstructed from the available tracking data). The latency of the TLE set is around 12 hours. Cryosat-2 TLE data is updated on a daily basis, it is considered to be a low accuracy data source that is only used as a backup facility in case there is no alternative source to provide an initial state vector. Relevant subsets of the TLE's are maintained at website **http://celestrak.com/NORAD/elements/**, and an automated perl script at the client work station retrieves the TLE data twice per day.
- A client linux workstation to update the earth orientation parameters from the IERS repositories at **www.iers.org** and **hpiers.obspm.fr**. The client linux workstation is also used to update magnetic field and solar flux tables from **ftp.ngdc.noaa.gov**.
- A client linux workstation on which DEOS/A&S installed the GEODYN-2 software package which consists of GEODYN-2E, GEODYN-2S and the tracking data formatter TDF. DEOS/A&S developed tools to convert native DORIS, SLR and CS2 quaternion data into input required for GEODYN-2.

2.1.2 Ground station coordinates for SLR and DORIS

POD depends on the availability of DORIS beacon and SLR tracking station coordinates. The International Terrestrial Reference Frame (ITRF) is a reference system which provides estimated coordinates and velocities of tracking stations. ITRF realizations are frequently updated and DEOS/A&S selected the most recent known coordinates for ground stations within the ITRF2008 reference system, see also **ftp://itrf.ensg.ign.fr/pub/itrf/**.

The majority of the DORIS ground station coordinates originate can be found within ITRF2008. For the DORIS ground station coordinates that were not provided in ITRF2008 DEOS/A&S selected the ITRF2005 coordinates. However, both

for SLR and DORIS, ITRF2005 has some deficiencies and extensions (scaled versions) are used during POD, see also *Willis et al.* [2009] and *Ries* [2010].

The biggest deficiency is that ITRF2005 coordinates are not available for quite a number of DORIS stations, because only stations through the end of 2005 are included while newer stations are not included in this reference frame solution. After 2006, the number of DORIS antenna's has rapidly grown, hence it is important to update the coordinates. Moreover, due to more recent studies and methods, more accurate station position and velocities can be obtained after 2005.

For POD applications, also additional information, such as periods of equipment malfunctioning and discontinuities, are required. These considerations lead to DPOD2005, which is an extension of ITRF2005. It includes all new DORIS stations and is more reliable. The POD improvements rapidly and significantly increase after 2005. During the development phase for Cryosat-2 we encountered some issues with DPOD2005 version 1.4. These were communicated with the Institut de Physique du Globe de Paris and resulted in a new version: DPOD2005 version 1.5 (4 December 2009). Since this is the latest standard for POD with DORIS stations, this model is implemented during Cryosat's commissioning phase for DORIS stations one does not find in ITRF2008. To summarize the above discussion:

- ITRF2008 coordinate definitions were assumed for DORIS beacons: ADFB ARFB BADB BEMB CADB CHAB DIOB DJIB EASB EVEB FAIB FUTB GAVB GREB HBMB HEMB JIUB KETB KIUB KOLB LICB MAHB MALB MANB MATB METB MIAB MORB MSPB NOWB PDMB REUB REZB RIQB ROUB SAKB SALB SANB SCRB SPJB STJB SYPB THUB TLSB TRIB YASB YEMB.
- DPOD2005 v1.5 coordinates were assumed for DORIS beacons: AMVB BETB CIDB CRQB GR3B KRBB KRVB RILB SODB ASEB PAUB.
- ITRF2008 SLR tracking coordinate definitions were assumed for International Laser Ranging Service (ILRS) sites: 1824 1873 1884 1893 7080 7090 7105 7110 7119 7124 7237 7249 7308 7403 7501 7810 7821 7824 7825 7832 7839 7840 7841 7845 7941 8834.

2.1.3 Satellite attitude model

The spacecraft body fixed coordinate frame (SBF) of Cryosat-2 is nominally in a 6 degree pitch down configuration as explained in *Francis* [2005]. Furthermore there is a 4 degree yaw oscillation since 1 June, 2010. The used POD software does not provide the CS2 attitude law as a standard attitude model. For all satellites that don't follow known (read: coded within the current version of the POD software) attitude laws there will be a need to specify the attitude of the spacecraft by means of a set of quaternions where the orientation of the SBF is presented relative to J2000.

Star tracker quaternion data was provided by ESA. Each of the three star trackers on board the Cryosat-2 satellite provides quaternions in its own camera frame (SCF) relative to the inertial frame J2000. Internet access to the quaternion data is explained in section 2.1.1, on 5-10-2010 16:25 we retrieved 4582 star tracker attitude files which follow the format:

```
CS_OPER_STR[1-3]ATT_*.TGZ
```

Each package contains HDR and DBL files and software was developed by DEOS/A&S to decode the star tracker quaternions and the corresponding time

tags with the help of information provided by Christopher Götz at ESTEC Noordwijk, see also document *ESA* [2008].

The resulting quaternions provide the orientation of the SCF relative to the inertial reference system J2000. In order to apply these quaternions to POD further processing is required. Therefore we transform the star tracker observed quaternions into quaternions that describe the orientation of the SBF to J2000 for which DEOS/A&S used transformation matrices provided by Francesco Marchese at ESOC in Darmstadt, see also document *EADS* [2009]. The end result after transformation and data compression of the dense star camera dataset is a daily set of quaternions at 30 second intervals. Our daily sets of quaternions describe the orientation of the SBF relative to J2000. This set serves as input for the CS2 attitude model during POD.

In order to validate our generated spacecraft quaternions we confronted the interpolated set with a synthetic SBF retrieved from the Doris navigator orbit product as specified in section 2.1.1. This procedure allowed us to reconstruct the pitch, roll and yaw angles of Cryosat-2, and we confirmed that the satellite is in a 4 degree yaw steering mode since 28-5-2010 which is day number 148 in 2010, see figure 2.4. The period from launch up to 28-5-2010 is known for several orbit corrections and isolated periods where the satellite was operating in a reverse yaw condition as can be seen in figures 2.1, 2.2 and 2.3.

2.1.4 Solar radiation pressure model of Cryosat-2

The solar radiation pressure (SRP) model of Cryosat-2 is a box only model relying on input provided in document *Francis* [2005]. In total we defined 6 plates which are a macro model approximation of the full spacecraft. The radiation pressure scaling coefficient C_r was determined to be 0.92 which followed from an estimation of this coefficient in the first week of June 2010.

2.1.5 Antenna phase center definitions

Document *Francis* [2005] is used to specify the phase centers of the 401.25 MHz and 2036.25 MHz Doris antennas and the SLR cube corner coordinates. The 2 GHz phase center was chosen to represent carrier phase observations, and an ionospheric free combination is formed from the observations at both frequencies. For the SLR cube corner on Cryosat-2 we used a constant offset of 19 mm which is an approximation of the elevation dependent correction as explained in document *Goetz* [2006].

2.1.6 Satellite mass and center of gravity model

The position of the center of gravity within the satellite and its mass are frequently provided by ESOC, see also section 2.1.1. The frequency of the updates depends on maintenance maneuvers and the cold gas usage for the Attitude and Orbit Control Sub-System (AOCS). We receive maneuver updates by e-mail, furthermore they are provided by ESOC, see also section 2.1.1.

2.2 Precision orbit determination results for Cryosat-2

Given the fact that the CNES provides format 2.2 DORIS Doppler files since 1-June-2010 and that SLR data became available since 20-april-2010 we decided to

concentrate on the time frame 1-jun-2010 to 18-sep-2010. During POD we chose arcs to be not longer than 120 hours with an overlap of 24 hours. In addition we avoid to integrate equations of motion during a maneuver, see also section 2.1.6.

A second factor that determines the choice of the selected period is the availability of IERS bulletin B data which contain polar motion and length of day parameters. The update frequency of this product is 30 days which induces a latency in our POD procedures.

A third factor is the availability of final values for geo-magnetic intensity and solar flux constants which we retrieve from the National Geophysical Data Center (NGDC) via **ftp.ngdc.noaa.gov**. Both geophysical parameters are required within the atmospheric drag model and the solar radiation pressure model. Other acceleration models used during POD are:

- Potential coefficients of the Earth's gravity model: EIGEN-5C up to degree and order 70 including temporal gravity till degree and order 2.
- Tidal modeling: h_2 and l_2 from latest International Earth Rotation Service (IERS) standards, EGM96 ocean tides, including the FES2004 ocean load tide model for the SLR core station set.
- Thermospheric density model: MSIS-86
- Lunar and planetary ephemeris: DE/LE-200, planetary gravity constants as in IAU2000.
- Refraction modeling with the Marini Murray model. The ionospheric and tropospheric refraction for DORIS data is already provided by the CNES in their format 2.2 ten second averaged range rate product.
- General accelerations at one cycle per orbital revolution in the along-track and cross track direction at daily intervals. This model absorbs unmodelled accelerations on the spacecraft.
- The atmospheric drag scaling parameter (K_{drag}) is adjusted every twelve hours, the SRP model scaling parameter (C_r) is fixed at a constant value of 0.92.

In addition we specify a number of technique specific parameters during POD:

- The initial state vector for each arc was interpolated from the DORIS navigator orbit, and several adjustments are applied to reach convergence.
- DORIS measurement biases and tropospheric scaling parameters are solved by pass for each ground beacon.
- We solve for an arc dependent clock offset of the DORIS satellite receiver.
- Satellite ranging data is corrected for a 19 mm offset due to the phase center definition of the cube corner on Cryosat-2. ILRS tracking station number 1893 was corrected for a pass dependent range bias correction, 1873, 7090 and 7832 are corrected for pass dependent time biases.
- Dynamic editing techniques are used to remove spurious data-points in the SLR and the DORIS datasets. The relative weights in forming the normal equations involve an a priori choice of the observation standard deviation. To determine these weight we assumed an a priori standard deviation of 0.45 mm/s for DORIS and 5 cm for laser ranging data.
- Since the CNES did not apply beacon frequency offset corrections to the DORIS format 2.2 product we decided to use an a priori Doppler beacon fre-

quency offset table to assist the initialization of the dynamic editing procedures.

Table 2.1 shows the DORIS 10s average range rate residual statistics, and table 2.2 the SLR range rate residual statistics. Both tables apply to residuals for a selected arc. The conclusion is that the st.dev. of fit of the DORIS residuals becomes ≈ 0.4 mm/s while the SLR st.dev. of fit is near ≈ 3.0 cm st.dev. In table 2.3 we show the definitions of the arc begin and end times.

2.2.1 SLR-only and DORIS-only solutions

Our computed solutions significantly depend on information provided by the DORIS tracking system. To investigate this sensitivity we investigated a test arc starting at 27-jun-2010 0hr UTC running to 30-jun-2010 0hr UTC. In this test period there is strong SLR coverage, and we can compute a SLR-only solution.

The difference of the SLR only solution compared to CNES POE solution shows the following standard deviations: cross-track: 8.28 cm, radially: 3.29 cm and along track: 11.98 cm while the standard deviation of the three-dimensional difference is 14.93 cm. The DORIS-only solution show the following statistics: cross-track: 5.57 cm, radially: 1.31 and along track: 3.88 cm. The standard deviation of the three-dimensional difference to the CNES POE orbit is 6.92 cm. For the DORIS+SLR combination solution we get for the test arc: cross-track: 4.11 cm, radial: 1.31 cm and along track: 6.19 cm, in 3D the standard deviation is 7.55 cm.

The SLR-only solution is of course worse than what is typically obtained by a DORIS-only or a DORIS+SLR solution, but the SLR-only is a possible option to consider if for some reason Cryosat-2 would ever lose DORIS tracking support. For the ERS-1 mission this was the situation due to the early demise of the PRARE tracking system. For ERS-1 DEOS/A&S was able to combine SLR tracking with the altimeter cross-over data to improve the trajectory of ERS-1.

2.3 External Orbit validation of Cryosat-2

During the commissioning phase the CNES produced MOE and POE orbits for Cryosat-2 while the on board flight receiver software (DIODE) produced real-time solutions. We retrieved these data from the CALVAL server as described in section 2.1.1 and computed differences as indicated in tables 2.4, 2.5 and 2.6.

On 30 June 2010 between 12:58:26 and 13:48:26 the DIODE system experienced an anomaly which was reported by CNES to ESA. The DIODE system returned online on 13:48:26 UTC, the 3D error of the DIODE navigator solutions reduced to less than 10 m on 14:46:26 UTC. This anomalous situation explains the extreme difference between our solutions and the DIODE navigation solution on 30 June 2010 which is in the overlap of arcs 06/26 and 06/30.

When we omit both anomalous arcs the differences between the Diode navigator orbits and our solutions is 9.36 cm st.dev. in the direction normal to the orbital plane which we will refer to as the cross-track direction. In the radial direction we find an agreement to within 9.43 cm st.dev, and in the in the traverse or along-track direction we get 14.87 cm st.dev, see also table 2.4. This means that a real-time solution of the DIODE system is better than the pre-flight specification of the TOPEX/Poseidon altimeter which was launched by the National Aeronautics and Space Administration (NASA) in 1992. The DIODE navigator orbits are a part of the AOCS on the Cryosat-2 mission, initialization of the star cameras

depends on the DIODE navigator orbits, and also the satellite reference time is controlled by the ultra stable oscillator of the Doris system.

The CNES provided two additional products which are referred to as the MOE and the POE orbits. The MOE orbits agree to within 4.46 cm, 2.04 and 6.70 cm st.dev. in respectively the cross-track, the radial and the along-track direction. In table 2.5 we show the individual mean and standard deviations for the arcs that we computed between 1-jun-2010 to 18-sep-2010. For the POE orbits we see an average standard deviation of 4.97 cm, 1.82 cm and 6.29 cm in the cross-track, the radial and the along track direction, the POE version of table 2.5 is shown in table 2.6. The MOE orbits are a clear improvement over the DIODE navigator product and they are available within one day, the POE orbits have a latency of a month, the POE orbits show a 10% improvement in the radial residuals compared to the MOE's.

2.4 Conclusions and recommendations

During the commissioning phase DEOS/A&S studied the complete POD processing chain which involves retrieval of satellite tracking data, spacecraft attitude data, and geophysical model data, including auxiliary data from various sources. In the following we will briefly summarize the main findings during the commissioning phase.

We demonstrated that the best agreement was found with the CNES POE orbits. When we compare our arcs to these products we see an average standard deviation of 4.97 cm, 1.82 cm and 6.29 cm in the cross-track, the radial and the along track direction, the residuals by arc are shown in table 2.6. Our DORIS measurement residuals are in the order of 0.4 mm/s for 10s averaged range rates, for the SLR residuals we have 3.0 cm st.dev.

We see already that the combination of SLR and DORIS orbits yields somewhat deteriorated solutions compared to the DORIS only solution when we compare both our products with the CNES POE solution. This is work in progress, because it could point to issues that we may need to be improved in the operational phase of Cryosat-2. Our recommendations for further research during the operational phase are:

- Improve on relative observation data weighting between SLR and DORIS.
- Improve phase center offset maps of the DORIS antenna on Cryosat-2. Is there a dependency on the azimuth and elevation on the satellite looking at a DORIS ground beacons? Investigate also the phase center maps of the individual ground beacons.
- Investigate whether there are unresolved coordinate offsets on both the DORIS beacons and the SLR tracking stations.
- Investigate the need to refine the SRP model used during POD, is there a need to improve the C_r constant?
- Is a more aggressive parameterization of the drag and the 9 parameter general acceleration model an option? For a discussion see section 2.4.1.
- Can we confirm or improve accuracy of the Cryosat-2 orbits by means of minimization of crossover residuals seen by the SIRAL LRM radar?

2.4.1 Variations in K_{drag} due to thermospheric density changes.

During POD we solve for 12 hourly values of the drag model scaling parameter K_{drag}. The solved for K_{drag} values during POD are an approximation that depends on the used thermospheric density model (MSIS-86) and the solved for K_{drag} should not be confused with the physical value of C_d of Cryosat-2 which depends on the shape of Cryosat-2. The thermosphere density model depends on the intensity of the solar flux and charged particles emitted by the Sun which are captured in the Earth's magnetosphere. Proxy relations are modelled in MSIS-86. These relations enable to approximate the density of the thermosphere to variations in the solar flux and the charged particle intensity for which the geomagnetic index K_p provided by the NGDC is taken as a reference.

The implementation in MSIS-86 takes into account a solar flux constant represented by the flux received at 2800 MHz or 10.7 cm (hence called F10.7) and 3 hourly values of the geo-magnetic indices K_p which are both provided by the NGDC. If the proxy relations in MSIS-86 are accurately implemented then one would see a constant drag model scaling parameter K_{drag} over time, yet in reality the implementation in MSIS-86 is an approximation so that there are excursions in the K_{drag} values which reflect the inability of the used drag model to capture the accelerations seen by Cryosat-2 as a result of thermospheric density variations.

An example of the behavior of the drag model scaling parameter K_{drag} which we solve for during POD is shown in the upper panel of figure 2.5. At the beginning of the analyzed period we saw K_{drag} values around 1.5, and near the end of our analyzed period we ended up over 2.0. To visualize the relation to the Earth's geomagnetic intensity the K_p parameter retrieved from the NGDC is plotted in the bottom panel of figure 2.5.

An interesting part of the plot is the excursion on days 215-217 in 2010 which corresponds to 3-aug-2010 till 5-aug-2010. In this time frame there is a brief energetic burst of charged particles from the Sun. These charged particles interact with the Earth's geomagnetic field which is reflected in the K_p parameters retrieved from the NGDC. Remarkable is the correspondence between the above described burst of energetic particles and the change of K_{drag} which comes from a background level of around 2 to about 3.5 during the storm.

The question is now how atmospheric drag and solar radiation pressure will behave in the coming years, and in particular, whether the presently pursued scheme for modelling drag and generalized acceleration parameters including the SRP model used for the satellite can be maintained, or whether there is need for a micromodel approach to improve the SRP model, including a more aggresive way of parameterizing K_{drag} and generalized acceleration parameters during POD.

2.5 Acknowledgments

The GEODYN-2 software is kindly provided by the NASA Goddard Space Flight Center, Greenbelt, Maryland.

2.6 Tables and figures

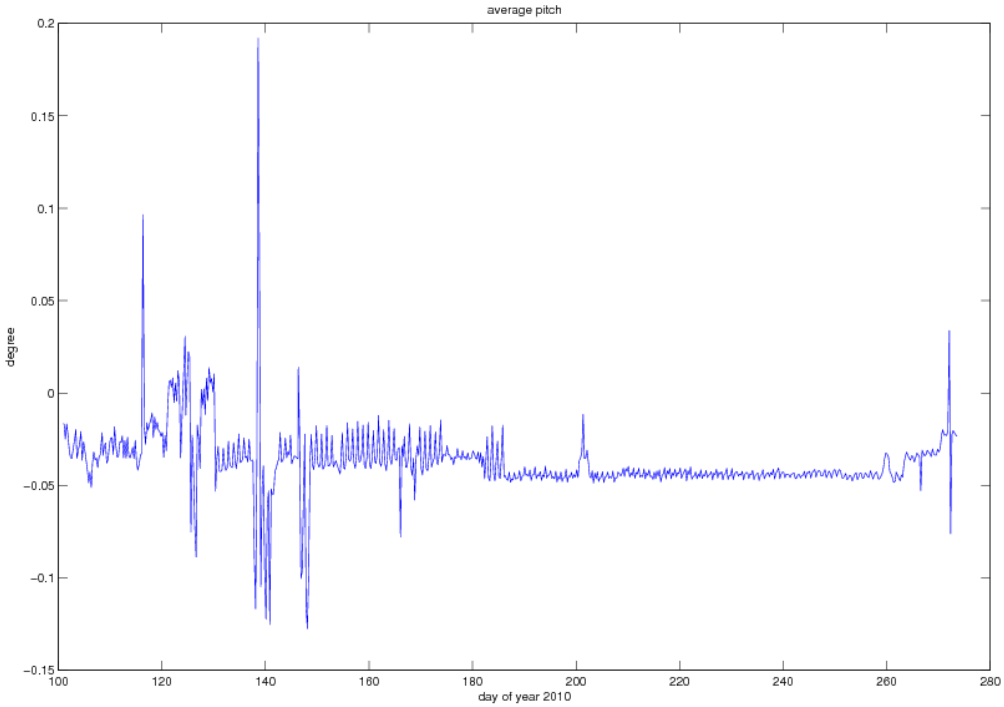

Figure 2.1 Three hourly averaged pitch angle as a function of the day of year 2010. For reference, day number 100 refers to 10-apr-2010, day number 280 corresponds to 7-oct-2010.

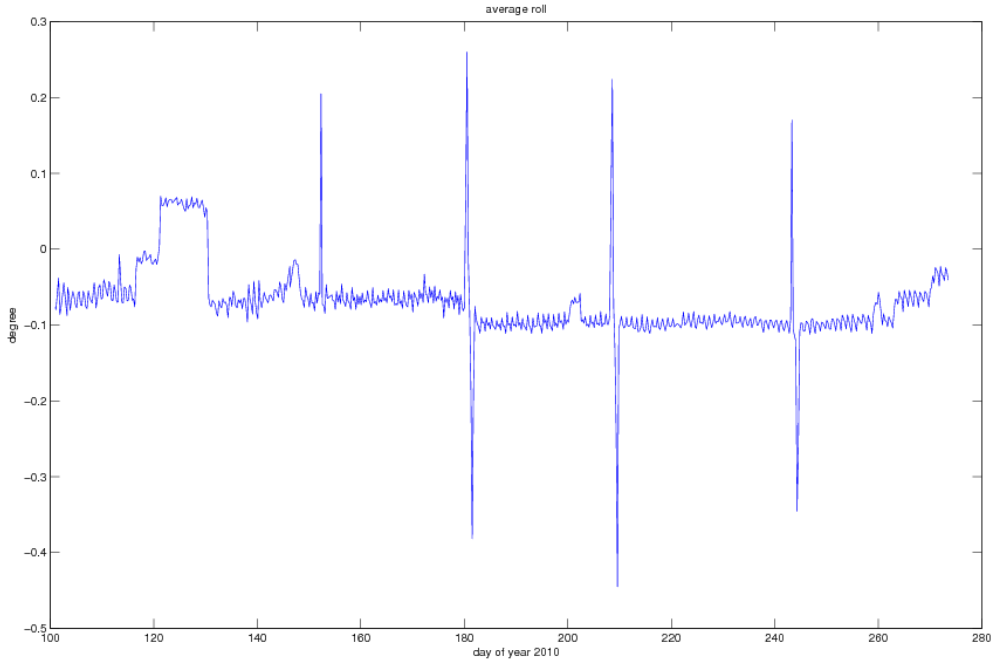

Figure 2.2 Three hourly averaged roll angle as a function of the day of year 2010. For reference, day number 100 refers to 10-apr-2010, day number 280 corresponds to 7-oct-2010.

Date	#s	#p	#d1	#d2	st.dev.
06/01	50	1105	44227	40850	0.4002
06/05	49	1312	53276	52046	0.4029
06/10	48	1099	43570	41061	0.4057
06/15	48	627	24669	23816	0.3957
06/18	48	1134	44871	41982	0.3971
06/22	48	1099	43863	41479	0.4094
06/26	48	1091	44065	40739	0.4056
06/30	48	1075	43192	41152	0.3907
07/05	46	1043	42294	39880	0.4008
07/09	47	1063	43119	40463	0.4197
07/13	48	1079	43417	39848	0.4126
07/17	49	901	35282	33925	0.4075
07/19	49	1111	44323	39343	0.4085
07/24	49	1098	43814	39024	0.4074
07/28	48	1077	43170	39553	0.3998
08/01	48	1071	43592	39177	0.4040
08/05	48	1059	42721	40267	0.4095
08/09	49	1080	42916	38565	0.4117
08/13	46	1059	42117	37198	0.4014
08/17	47	1037	41849	38573	0.4056
08/21	48	1066	42909	39032	0.4002
08/25	48	1092	43908	40650	0.3928
08/29	48	1078	43954	40563	0.3962
09/02	48	1097	44496	40689	0.3967
09/06	48	1074	43562	40424	0.3988
09/10	47	1080	43036	39624	0.3885
09/14	48	1062	42095	38127	0.3928

Table 2.1 DORIS 10s averaged range rate statistics by arc. Column date refers to an arc definition which is explained in table 2.3, #s indicates the number of used DORIS ground beacons, #p refers to the number of passes, #d1 and #d2 are the number of observation records before and after editing, mean and st.dev. refer to an average and a standard deviation of the DORIS measurement residuals in mm/s.

Date	#s	#p	#d1	#d2	st.dev.
06/01	16	47	653	593	2.3196
06/05	16	61	1002	926	2.8512
06/10	12	48	606	475	4.1304
06/15	10	27	293	279	2.0601
06/18	11	33	436	343	2.9754
06/22	14	66	943	875	3.3476
06/26	14	67	1092	968	3.0435
06/30	17	80	1143	915	2.5934
07/05	17	73	943	844	2.6489
07/09	15	73	1101	1005	3.0482
07/13	15	65	873	822	2.9016
07/17	13	44	458	407	3.1122
07/19	18	78	981	889	3.2795
07/24	15	52	672	482	3.5175
07/28	15	62	824	534	2.9503
08/01	17	91	1093	743	2.8172
08/05	16	67	827	547	3.6264
08/09	15	73	912	740	3.1418
08/13	18	61	672	572	2.8907
08/17	16	66	911	770	3.8227
08/21	19	87	1004	745	2.9597
08/25	18	62	769	445	2.6508
08/29	19	92	1154	941	2.5222
09/02	16	76	993	729	2.9710
09/06	16	81	1034	545	3.6066
09/10	18	85	1148	901	3.6591
09/14	16	61	804	680	3.7988

Table 2.2 Satellite laser ranging statistics by arc. Column date is defined in table 2.3, #s indicates the number of used SLR tracking stations, #p refers to the number of passes, #d1 and #d2 are the number of observation records before and after editing, mean and st.dev. refer to an average and a standard deviation of the SLR measurement residuals in cm.

Date	start date	start time	stop date	stop time
06/01	1-jun-2010	00:00:26	6-jun-2010	00:00:26
06/05	5-jun-2010	00:00:26	11-jun-2010	00:00:26
06/10	10-jun-2010	03:00:26	15-jun-2010	03:00:26
06/15	15-jun-2010	03:15:26	18-jun-2010	01:15:26
06/18	18-jun-2010	01:15:26	23-jun-2010	01:15:26
06/22	22-jun-2010	00:00:26	27-jun-2010	00:00:26
06/26	26-jun-2010	00:00:26	1-jul-2010	00:00:26
06/30	30-jun-2010	00:00:26	5-jul-2010	00:00:26
07/05	4-jul-2010	00:00:26	9-jul-2010	00:00:26
07/09	8-jul-2010	00:00:26	13-jul-2010	00:00:26
07/13	12-jul-2010	00:00:26	17-jul-2010	00:00:26
07/17	16-jul-2010	12:37:26	20-jul-2010	12:37:26
07/19	20-jul-2010	12:37:26	25-jul-2010	12:37:26
07/24	24-jul-2010	00:00:26	29-jul-2010	00:00:26
07/28	28-jul-2010	00:00:26	2-aug-2010	00:00:26
08/01	1-aug-2010	00:00:26	6-aug-2010	00:00:26
08/05	5-aug-2010	00:00:26	10-aug-2010	00:00:26
08/09	9-aug-2010	00:00:26	14-aug-2010	00:00:26
08/13	13-aug-2010	00:00:26	18-aug-2010	00:00:26
08/17	17-aug-2010	00:00:26	22-aug-2010	00:00:26
08/21	21-aug-2010	00:00:26	26-aug-2010	00:00:26
08/25	25-aug-2010	00:00:26	30-aug-2010	00:00:26
08/29	29-aug-2010	00:00:26	3-sep-2010	00:00:26
09/02	2-sep-2010	00:00:26	7-sep-2010	00:00:26
09/06	6-sep-2010	00:00:26	11-sep-2010	00:00:26
09/10	10-sep-2010	00:00:26	15-sep-2010	00:00:26
09/14	14-sep-2010	00:00:26	19-sep-2010	00:00:26

Table 2.3 Start and stop dates and times by arc. Column ”Date” is the reference date specified as month/day in 2010 that is used in tables 2.1, 2.2 2.4 2.5 and 2.6.

Date	#h	mean1	stdev1	mean2	stdev2	mean3	stdev3	#v
06/01	120	0.004	0.082	-0.035	0.095	-0.165	0.171	6426
06/05	143	0.006	0.099	-0.039	0.133	-0.162	0.235	9158
06/10	120	0.007	0.104	-0.032	0.098	-0.100	0.178	7468
06/15	70	0.007	0.102	-0.039	0.090	-0.129	0.129	4340
06/18	120	0.005	0.112	-0.040	0.100	-0.167	0.133	7580
06/22	120	0.008	0.111	-0.039	0.105	-0.112	0.154	7565
06/26	120	0.001	1.055	0.007	2.036	-1.065	10.930	7574
06/30	120	-0.001	1.051	0.011	2.031	-1.080	10.896	7620
07/05	120	0.005	0.088	-0.039	0.101	-0.123	0.165	7716
07/09	120	0.004	0.094	-0.041	0.095	-0.130	0.158	7721
07/13	120	0.003	0.097	-0.047	0.099	-0.145	0.151	7524
07/17	96	0.006	0.084	-0.044	0.101	-0.145	0.145	6067
07/19	120	0.007	0.089	-0.043	0.089	-0.137	0.130	7723
07/24	120	0.004	0.092	-0.048	0.089	-0.089	0.138	7702
07/28	120	0.002	0.109	-0.042	0.104	-0.138	0.184	7688
08/01	120	0.003	0.101	-0.040	0.078	-0.128	0.131	7598
08/05	120	0.004	0.087	-0.039	0.074	-0.085	0.131	7557
08/09	120	0.002	0.085	-0.042	0.086	-0.112	0.147	7558
08/13	120	0.002	0.090	-0.043	0.095	-0.164	0.124	7604
08/17	120	0.005	0.087	-0.045	0.089	-0.109	0.135	7702
08/21	120	0.002	0.097	-0.049	0.094	-0.125	0.147	7654
08/25	120	0.001	0.085	-0.039	0.087	-0.177	0.137	7603
08/29	120	0.002	0.076	-0.040	0.076	-0.173	0.114	7533
09/02	120	0.004	0.085	-0.035	0.094	-0.098	0.135	7534
09/06	120	0.002	0.098	-0.042	0.098	-0.147	0.149	7520
09/10	120	0.002	0.097	-0.041	0.092	-0.155	0.134	7460
09/14	120	0.003	0.109	-0.035	0.098	-0.126	0.135	7310

Table 2.4 Difference between the GEODYN solutions and the external ephemeris provided from the DIODE flight receive navigation system. Column date is defined in table 2.3, #h is the length in hours of the arc, mean1 and stdev1 refer to the average and the standard deviation in the normal to plane direction, mean2 and stdev2 are the average and the standard deviation in the radial direction, and mean3 and stdev3 refer to the flight direction. Units : meter. Column #v indicates the number of state-vectors used for the comparison.

Date	#h	mean1	stdev1	mean2	stdev2	mean3	stdev3	#v
06/01	120	0.003	0.049	-0.001	0.017	-0.085	0.076	7907
06/05	144	0.004	0.033	0.000	0.014	-0.072	0.051	9496
06/10	120	0.003	0.040	-0.000	0.017	-0.021	0.063	7946
06/15	70	0.003	0.037	-0.007	0.119	-0.055	0.311	4648
06/18	120	0.003	0.045	0.000	0.018	-0.083	0.056	7906
06/22	120	0.003	0.038	-0.000	0.015	-0.028	0.056	7907
06/26	120	0.002	0.045	-0.000	0.016	-0.014	0.050	7907
06/30	120	0.003	0.035	0.000	0.015	-0.039	0.047	7907
07/05	120	0.004	0.043	0.000	0.014	-0.035	0.045	7907
07/09	120	0.003	0.039	-0.001	0.018	-0.032	0.066	7907
07/13	120	0.004	0.042	-0.001	0.017	-0.041	0.056	7907
07/17	96	0.002	0.040	0.001	0.018	-0.049	0.064	6319
07/19	120	0.003	0.041	-0.000	0.021	-0.044	0.058	7908
07/24	120	0.003	0.063	-0.001	0.021	0.014	0.060	7907
07/28	120	0.002	0.036	-0.001	0.013	-0.052	0.043	7907
08/01	120	0.002	0.037	-0.001	0.014	-0.038	0.056	7907
08/05	120	0.002	0.040	-0.001	0.018	-0.000	0.066	7907
08/09	120	0.003	0.045	-0.001	0.020	-0.016	0.067	7907
08/13	120	0.002	0.058	-0.001	0.016	-0.068	0.055	7907
08/17	120	0.002	0.041	-0.001	0.015	-0.015	0.056	7907
08/21	120	0.001	0.065	-0.000	0.016	0.013	0.063	7907
08/25	120	-0.001	0.044	-0.001	0.012	0.003	0.041	7781
08/29	120	-0.000	0.047	-0.001	0.015	0.004	0.054	6338
09/02	120	-0.001	0.057	0.000	0.016	0.073	0.055	7907
09/06	120	-0.003	0.053	-0.000	0.016	0.041	0.060	7907
09/10	120	-0.003	0.055	-0.000	0.015	0.019	0.052	7907
09/14	120	-0.002	0.040	-0.001	0.015	-0.019	0.082	7907

Table 2.5 Difference between the GEODYN solutions and the intermediate orbit ephemeris (MOE's) provided by the CNES. Column date is defined in table 2.3, #h is the length in hours of the arc, mean1 and stdev1 refer to the average and the standard deviation in the normal to plane direction, mean2 and stdev2 are the average and the standard deviation in the radial direction, and mean3 and stdev3 refer to the traverse direction. Column #v indicates the number of state-vectors used for the comparison.

Date	#h	mean1	stdev1	mean2	stdev2	mean3	stdev3	#v
06/01	120	0.002	0.056	-0.000	0.014	-0.069	0.051	7907
06/05	144	0.003	0.061	-0.000	0.014	-0.067	0.057	9496
06/10	120	0.002	0.069	-0.001	0.019	-0.018	0.072	7946
06/15	70	0.001	0.040	-0.000	0.015	-0.030	0.052	4648
06/18	120	0.002	0.054	-0.001	0.015	-0.070	0.049	7906
06/22	120	0.002	0.057	-0.001	0.017	-0.023	0.074	7907
06/26	120	0.002	0.053	-0.000	0.019	-0.005	0.062	7907
06/30	120	0.003	0.044	-0.001	0.020	-0.028	0.056	7907
07/05	120	0.003	0.042	-0.001	0.016	-0.033	0.051	7907
07/09	120	0.003	0.048	-0.001	0.020	-0.034	0.090	7907
07/13	120	0.004	0.046	-0.002	0.021	-0.033	0.068	7907
07/17	96	0.001	0.037	-0.000	0.022	-0.050	0.078	6319
07/19	120	0.002	0.048	-0.002	0.020	-0.031	0.069	7908
07/24	120	0.003	0.053	-0.002	0.023	0.022	0.068	7907
07/28	120	0.003	0.050	-0.001	0.017	-0.039	0.052	7907
08/01	120	0.001	0.040	-0.001	0.018	-0.024	0.065	7907
08/05	120	0.002	0.061	-0.001	0.020	0.018	0.070	7907
08/09	120	0.003	0.071	-0.002	0.021	-0.003	0.069	7907
08/13	120	0.002	0.049	-0.001	0.015	-0.062	0.055	7907
08/17	120	0.001	0.050	-0.001	0.022	-0.003	0.071	7907
08/21	120	0.000	0.039	-0.000	0.019	-0.008	0.058	7907
08/25	120	-0.001	0.044	-0.001	0.016	-0.071	0.053	7907
08/29	120	-0.000	0.034	-0.001	0.014	-0.080	0.056	7907
09/02	120	-0.001	0.047	-0.000	0.021	-0.008	0.067	7907
09/06	120	-0.002	0.049	-0.001	0.017	-0.030	0.058	7907
09/10	120	-0.002	0.040	-0.001	0.018	-0.049	0.050	7907
09/14	120	-0.002	0.062	-0.000	0.020	-0.036	0.067	7781

Table 2.6 Difference between the GEODYN solutions and the precision orbit ephemeris (POE's) provided by the CNES. Column date is defined in table 2.3, #h is the length in hours of the arc, mean1 and stdev1 refer to the average and the standard deviation in the normal to plane direction, mean2 and stdev2 are the average and the standard deviation in the radial direction, and mean3 and stdev3 refer to the traverse direction. Column #v indicates the number of state-vectors used for the comparison.

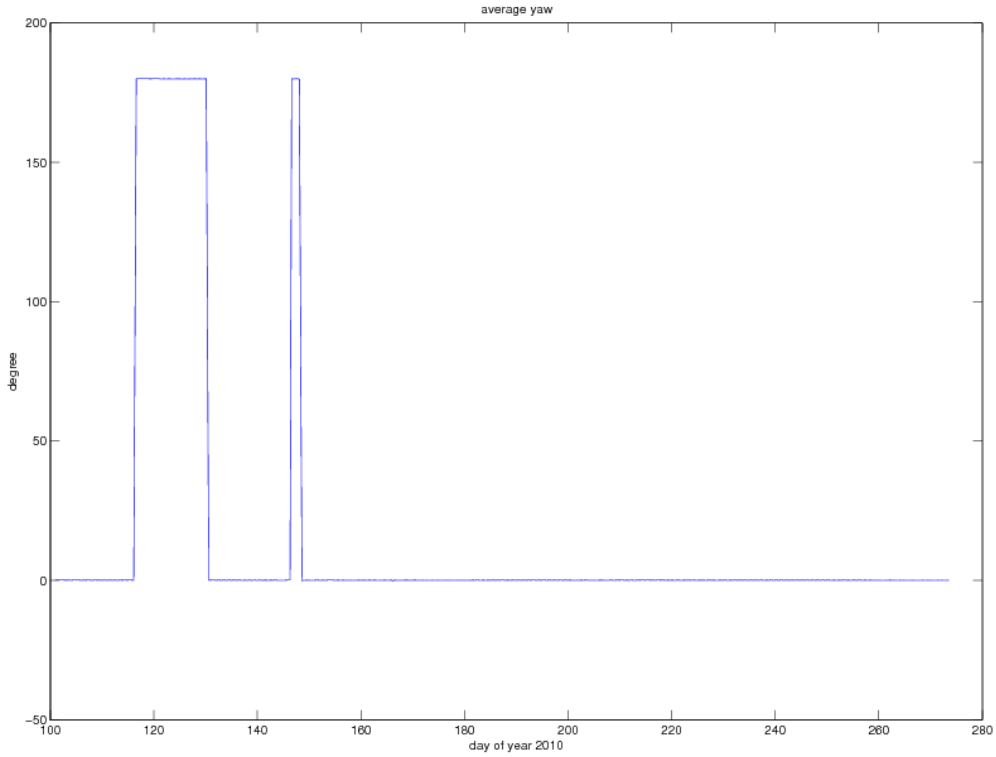

Figure 2.3 Three hourly averaged yaw angle as a function of the day of year 2010. For reference, day number 100 refers to 10-apr-2010, day number 280 corresponds to 7-oct-2010.

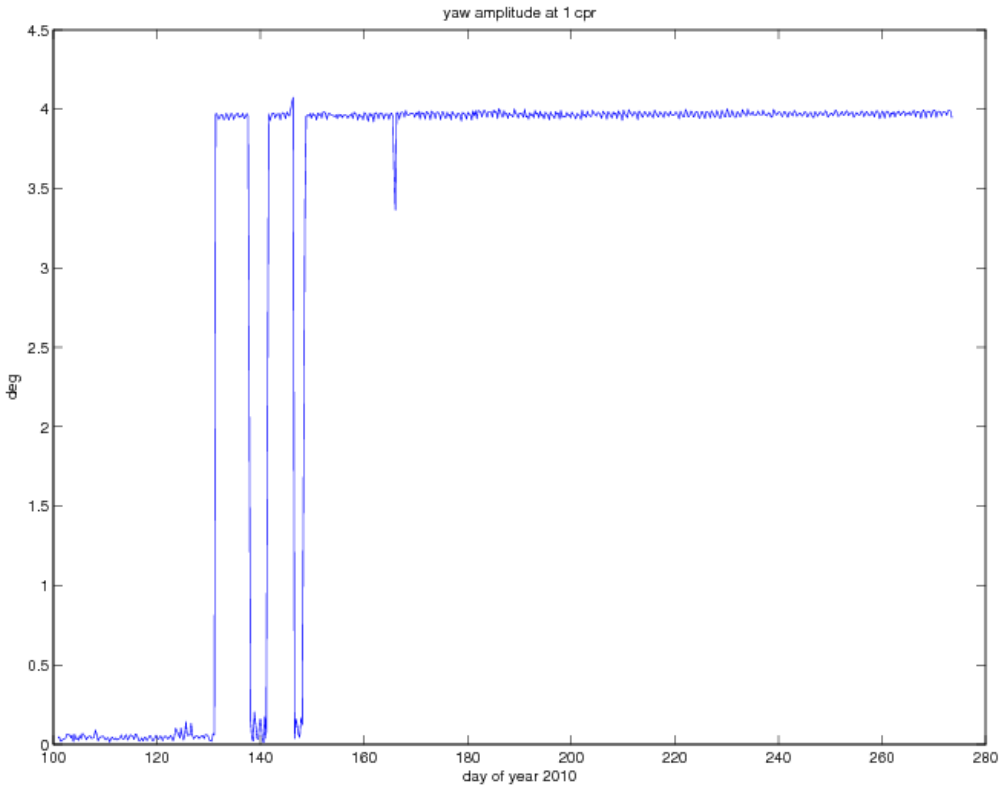

Figure 2.4 Three hourly averaged yaw amplitude at orbital period as function of the day of year 2010. For reference, day number 100 refers to 10-apr-2010, day number 280 corresponds to 7-oct-2010.

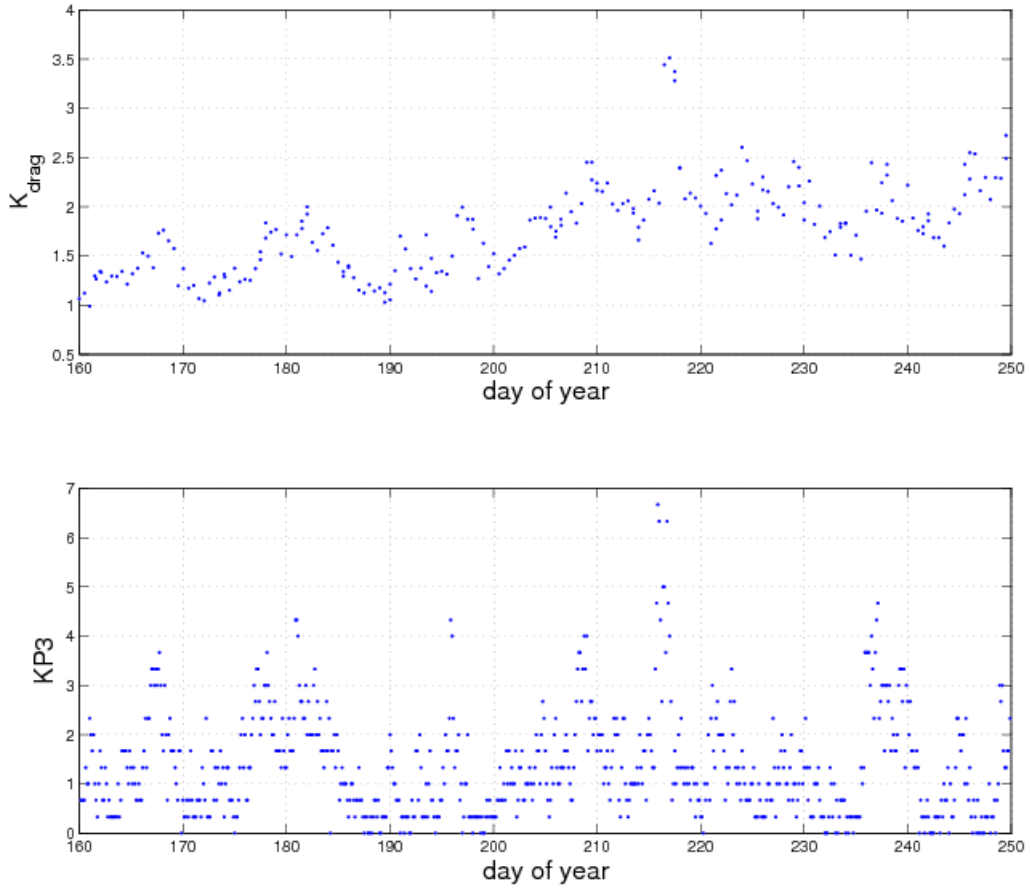

Figure 2.5 Top panel, behavior of the atmospheric drag model scaling parameter K_{drag} as a function of the day in year 2010, bottom panel, three hourly K_p values retrieved from the NGDC. For reference, day number 160 refers to 9-jun-2010, day number 250 corresponds to 7-sep-2010.

Chapter *3*

WP 520: Indirect Calibration of SIRAL - Commissioning Phase

This section deals with the work conducted for the calibration and validation of the CryoSat-2 Ocean product, or Low Resolution Mode (LRM) data and provides the status at the end of the Commissioning Phase. (The LRM level 1b data format is described in *ACSL1b* [2009] and the level 2 data in *ACSL2* [2009].) This work, referred to as WP 520 in the "CryoSat-2 Precise Orbit Determination and Indirect Calibration of SIRAL" project plan, entailed the analysis and identification of systematic errors in the CryoSat-2 LRM observations, first estimation of range bias and the preliminary comparison with other operational altimeter satellites. A full cross-calibration with Envisat, Jason-1 and Jason-2 though could not be performed due to not yet resolved (but understood and soon to be resolved) bugs in the ground processing of the raw altimeter product. In spite of this, already very useful conclusions can be drawn from the analyses that at the same time helped to improve the ground processing chain. We see this "exercise" as work in progress and expect a continued research on data quality, range bias and time tag bias in the Operational Phase. We acknowledge the need for a persistent monitoring of these biases in time to be able to provide insight in drift, which could be important to be taken into account when using the data for the investigation of long-term changes like sea level change, and or ice topography/volume change. In addition, we expect that the altimeter (range) data can be used to assess the radial orbit accuracy by generating crossover statistics which is a standard technique that we apply for ERS-1/2, Envisat, Topex/POSEIDON, Jason-1/2 and GFO. This is now planned for the Operational Phase. Meanwhile DEOS debugged its in-house software (RADS and applications) to address the latest issues with the CryoSat data. At this point, we are convinced that there is no need for adding altimeter data as tracking information to the set of DORIS and SLR because these already provide very consistent and accurate orbits. Altimetry is useful if there would be a shortage of tracking data, though the direct danger of adding altimetry would be leakage of ocean dynamics into the orbit.

3.1 Work package tasks, inputs and outputs

Tasks defined under WP 520:

- LRM altimeter bias and time tag estimation in POD
- LRM altimeter bias and time tag estimation by comparison with altimeter data from other satellites

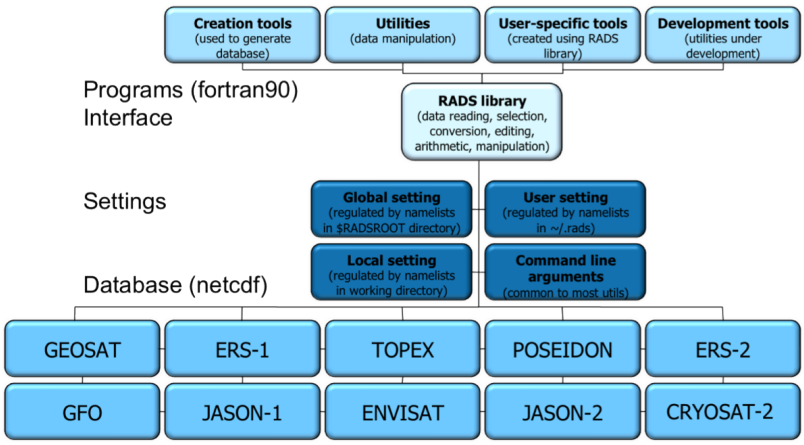

Figure 3.1 The TUDelft/NOAA/Altimetrics RADS system in the year 2010 with CryoSat-2 included

For this we have the following inputs:

- CryoSat-2 infrastructure from WP 120 and 310
- SIRAL LRM observations
- Directives from WP 120

And the following output:

- SIRAL LRM bias and time tag estimates
- Reports including accuracy assessments

3.2 Indirect calibration

The baseline indirect calibration methodology established in the readiness report (Development Phase) is defined by the following methods:

- Comparing range measurements and relevant range delays (tropo, iono), wave height, and wind speed, both internally (from global overall analysis and single-satellite crossovers) and externally (from global overall analysis and dual-satellite crossovers, *i.e.* CryoSat-2 crossings with other satellites).
- Verification/validation of time tag biases and drifts, realized through minimization of crossover height differences.

In support of this, geophysical and media correction algorithms including (ocean) tides and sea state bias (SSB) have to be investigated. Other supporting methods include sea surface topography time series, normal point analysis, and mean sea surface model residual analysis (comparing scientific results from different satellites). In the introduction we already indicated that this will take place in the Operational Phase and that we here focus on the sanity of the data in support of the ground processing chain (from Level-0, via Level-1b, up to Level-2).

For all our calibration and validation work we employ the Radar Altimeter Database System (RADS) initiated at DEOS/TUDelft and further developed by DEOS, NOAA and Altimetrics LLC ([*Naeije et al.*, 2002, 2007, 2008]). Figure 3.1

shows the general concept of RADS. This system not only contains all historical altimeter data up to date but also facilitates easy access, cross-calibration and data analysis ("system tools"). In 2009 the system was overhauled, software totally rewritten in Fortran 90 and now storing the data in NETCDF format. The actual work in frame of our project mainly consisted of transferring and by that converting CryoSat-2 LRM Level-2 data to the native RADS (V3) format; the "SIRAL reader" software. To ensure an operational work environment during commissioning phase the entire RADS system was ported to a separate multicore Xeon™ server running the SUSE Linux operating system. There is only a limited number of people that have access to this machine and the incoming data was shielded from other users.

3.3 Experiences with SIRAL LRM data

Purpose of validation is the confirmation that everything in the product is according to the product specification and within sensible predefined ranges. Calibration on the other hands seeks systematic biases to bring the product closer to reality, *e.g.* by inter-comparison with data from other missions and/or models. Additionally, we have checked the data against the description in the Level-2 products format specification, meaning that all slots in the data records have been examined. The check on the orbit parameters is dealt with in more detail in the "precise orbit determination" (POD) work of the project. During the commissioning phase we came across various errors, bugs, nonconformities and limitations in the SIRAL LRM level 2 data that we reported to ESA.

We focus our analysis on the time frame 29 August 2010 up to and including 29 September 2010, to make sure we use the "latest" data that already has gone through a number of ground track processing revisions during the commissioning phase, doesn't suffer from the ionospheric correction bug that was reported earlier (which affected not just the correction itself but also the actual height measurement) and also to have a stretch of data that was not disturbed by large orbit maneuvers. A 30-day period (referred to as "September 2010") was also chosen to have one complete subcycle of CryoSat's orbit. One full cycle is 369 days, which means the exact geographic location is revisited after 369 days, resulting in a 7.5 km track separation at the equator; for a sybcycle this is about 90 km. We screened the data for "open ocean" (surface type flag) and dry tropospheric, wet tropospheric and ionospheric correction not equaling zero.

In Figure 3.2 we plot the data fields for mispointing, dry troposphere, wet troposphere, ionosphere, inverse barometer, earth tide, ocean tide, and load tide as a function of latitude. Sigma's and means seem to compare very well with expected values (and shape of the plot) and values from the other altimeter satellites. Only the offset (mean) in the mispointing is of concern, though the standard deviation is well below 0.1 degrees, which indicates a stable platform.

We do the same in Figure 3.3, but now for polar motion, sea state, wave height, wind speed, mean sea surface, sigma-naught, corrected height, and sea surface anomaly. Here we do notice some unexpected behavior. For instance, for the sea state bias, the significant wave height and the wind speed, we find zero values most of the time. In case the values are not zero we see values that make perfectly sense, which we suspect come from properly re-tracked waveforms; so apparently, most of the time, the waveforms have not been re-tracked properly. We investigated this by plotting the locations of the data points that do have sen-

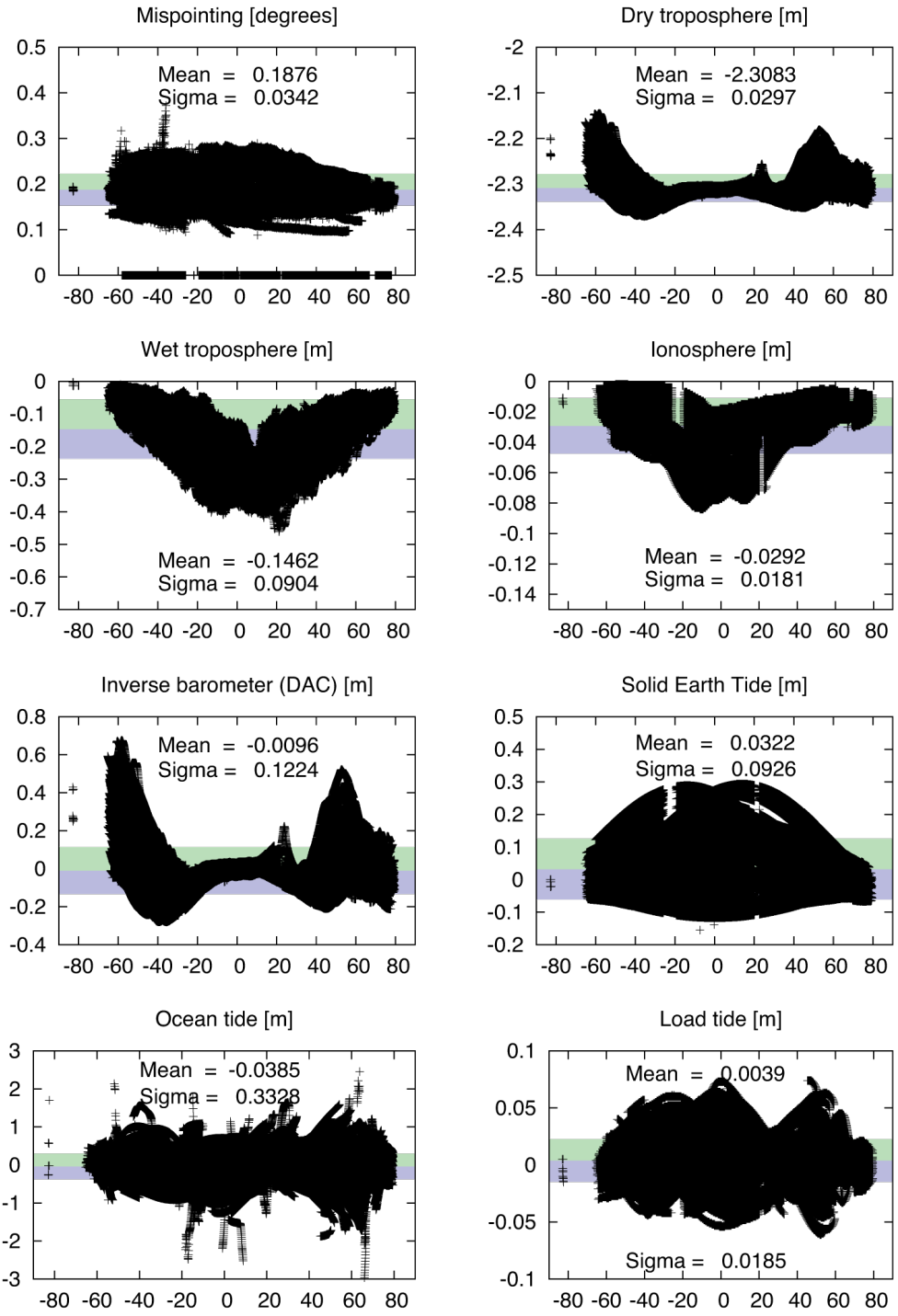

Figure 3.2 Status CryoSat-2 LRM data: data field contents for SIRAL LRM Level-2 during September 2010

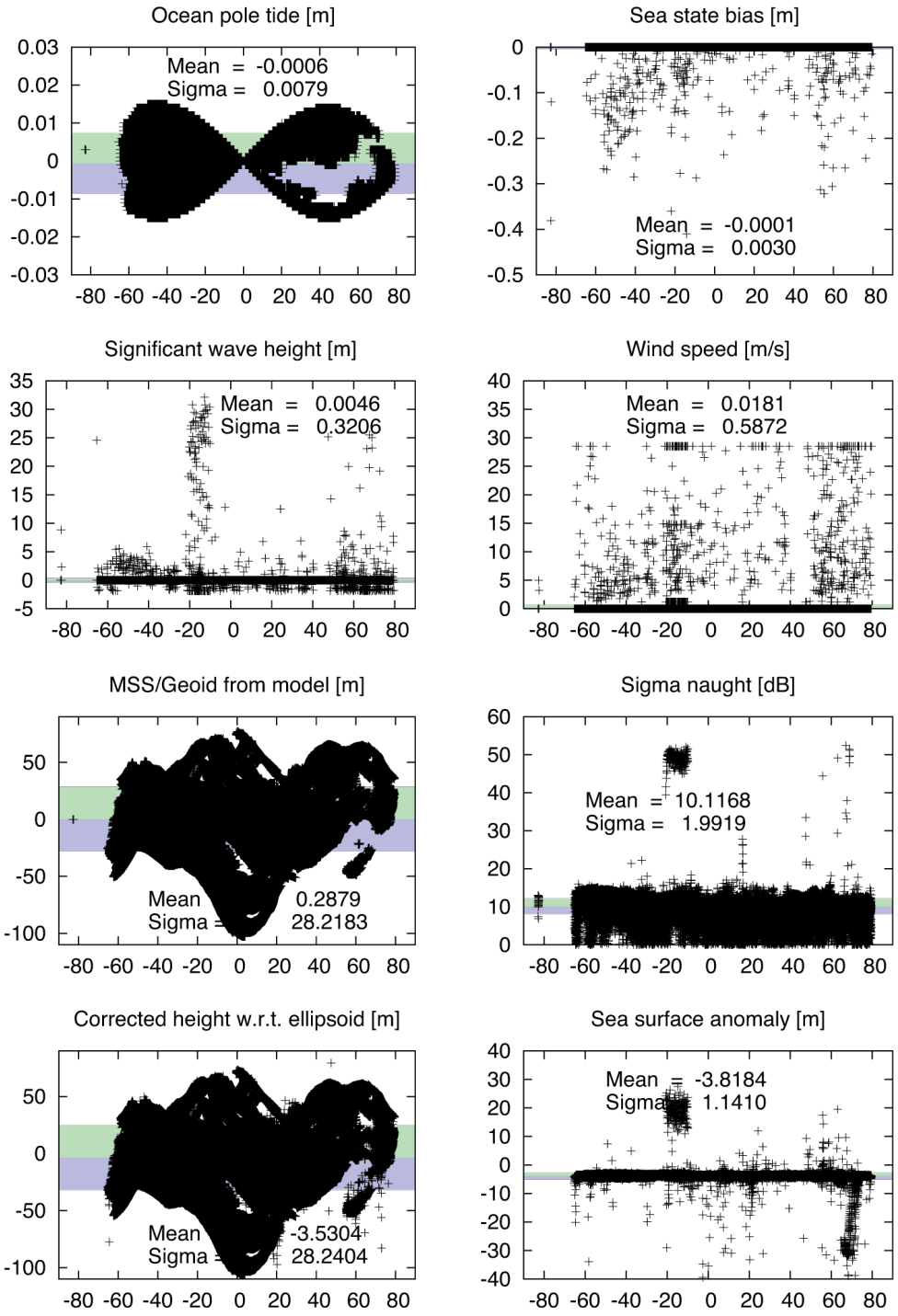

Figure 3.3 Status CryoSat-2 LRM data continued: remaining data field contents for SIRAL LRM Level-2 during September 2010

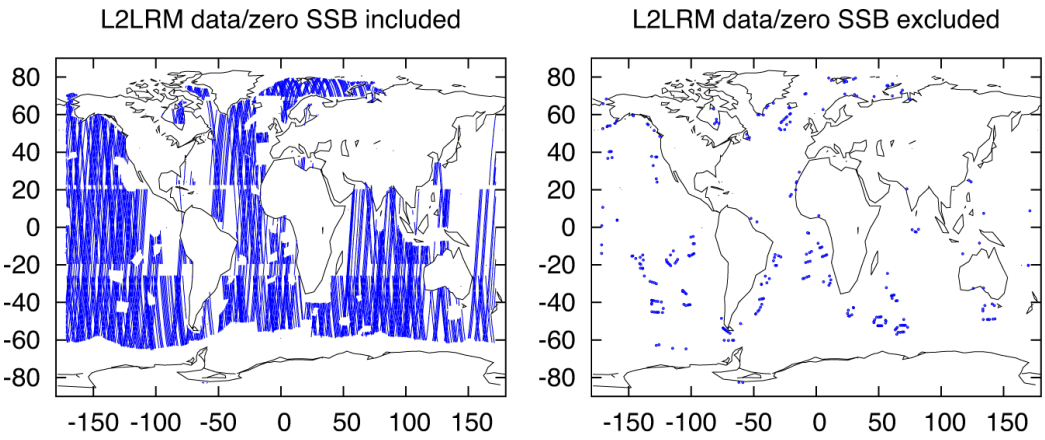

Figure 3.4 CryoSat-2 LRM geographical data coverage. Left: all open ocean data during September 2010, and right: excluding data with no sea state bias correction

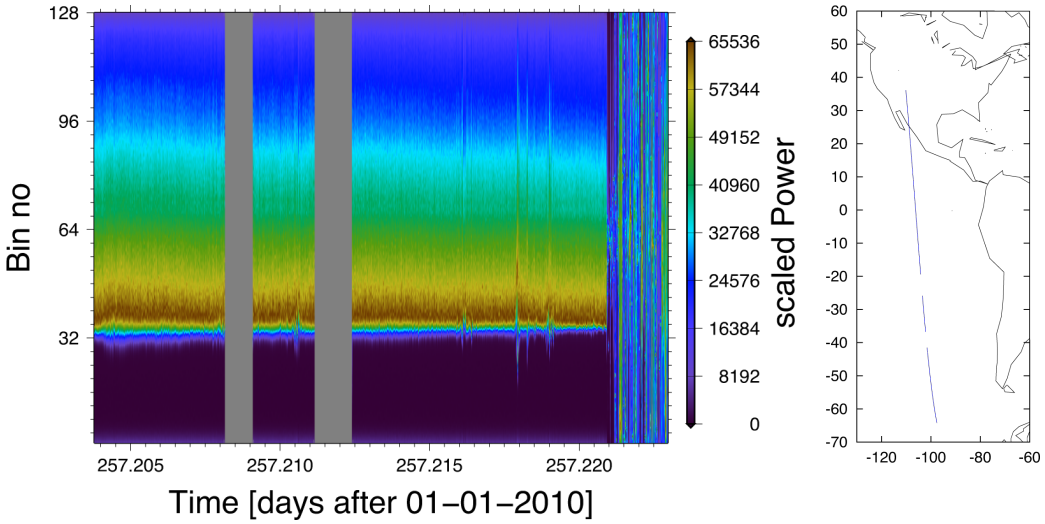

Figure 3.5 Left panel: scaled and averaged power of the echo waveform as function of time and bin, and right panel: the path the CryoSat satellite has followed, starting in the South, ascending to the North, and hitting land at the Mexican coast

sible values for these three parameters. This is shown in Figure 3.4. Comparing the right panel with the mode map for CryoSat we have to conclude that only sea state information (from the shape of the returned altimeter waveform) is available when the satellite changes mode from LRM to SAR and vice versa. This means that about 99% of the time the height that is transferred from the Level-1b product to the Level-2 product is the so-called OCOG height, where OCOG stands for Offset Centre of Gravity waveform parameterization), whereas it should have been the CFI re-tracker heights. This is supposed to be regulated by the PCONF parameter that checks the waveform quality in the L1b product, however it appears not to have been updated for actual data (as opposed to simulated data). This means that heights are not calibrated and are likely in error, and also detailed information on wave height and wind speed and by that of sea state is often missing. This has been acknowledged by both ESA and UCL, and an update that provides tuning of this PCONF allowing much more CFI re-tracked heights to enter the Level-2 product is foreseen before the end of 2010.

In Figure 3.5 we show that over the oceans the waveforms look very good

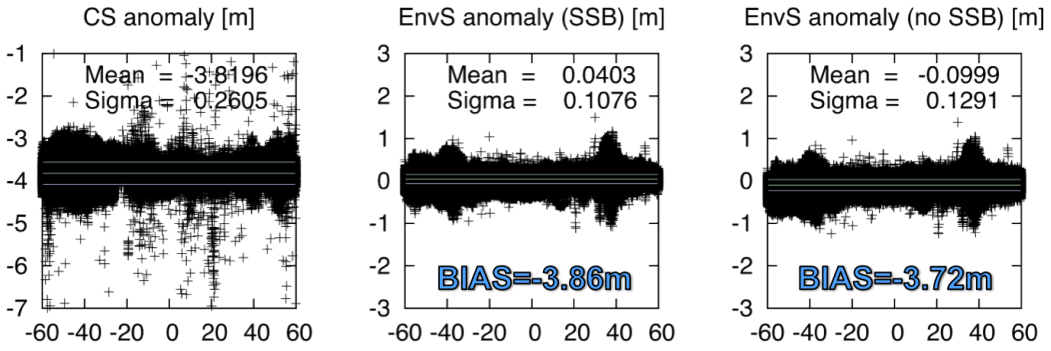

Figure 3.6 CryoSat-2 sea surface anomaly comparison with Envisat, either SSB applied or not applied

indeed, so it should not be a problem to generate consistent sea state biases from them, though the information is not there yet. On the other hand If SSB would remain a problem there are ways around it, including "home-made" re-tracking of the wave forms available in the L1b product, or the adoption of external wave data either from re-analysed wave models or from, in time and place, nearby satellites. Clearly the latter would result in a somewhat degraded product. The plot shows typical "Brown" returns over the ocean, as function of bin no starting with a stretch of very low values, than a sharp gradient to high values (leading edge), followed by a less sharper decline (tail). Obviously, the leading edge can be found around bin 32. Spikes in the waveform plot indicate locations where the altimeter interacts with seamounts and/or islands. The land returns by contrast are not Brown-model like, and dedicated (different) re-tracking algorithms would be more appropriate to deduce relief (if at all possible).

3.4 L2LRM: surface anomaly compared

In this section we will compare the sea surface anomaly from CryoSat-2 (CS) with that from Envisat (EnvS) to establish a first estimate of the range bias. It is important to know what the relative bias is of the altimeter data w.r.t. other altimeter satellites and also the absolute bias referenced to a reference ellipsoid. It will be clear that relative bias determination is not enough because any used cross-reference with other satellites may suffer from combined bias drifts. This is dealt with by repeated comparison of collocated altimetry and tide gauge data where at the same time the tide gauge is collocated with GPS. The latter will be discussed in the next chapter.

In Figure 3.3 the bottom right panel, we already looked at the so-called sea surface anomaly. This anomaly is defined as the corrected height w.r.t. the ellipsoid from which a mean sea surface model is subtracted (w.r.t. the same ellipsoid), in this case the CLS01 MSS. Corrected height means that all media corrections have been subtracted (this is already done in the Level-2 product), but we now know that the sea state bias is missing, and that there might be errors in the height due to the lack of re-tracking, furthermore, the SIRAL level 2 LRM product was not corrected for internal delays, cf. (Richard Francis, personal communication). Taking this into account we plot the 1-Hz value of sea surface anomaly in the left panel of Figure 3.6 and limit the area of investigation zonally between 60° North and South, to be able to make a direct comparison with both Envisat and Jason-2, which don't operate at the extreme latitudes CryoSat-2 does. We also introduce

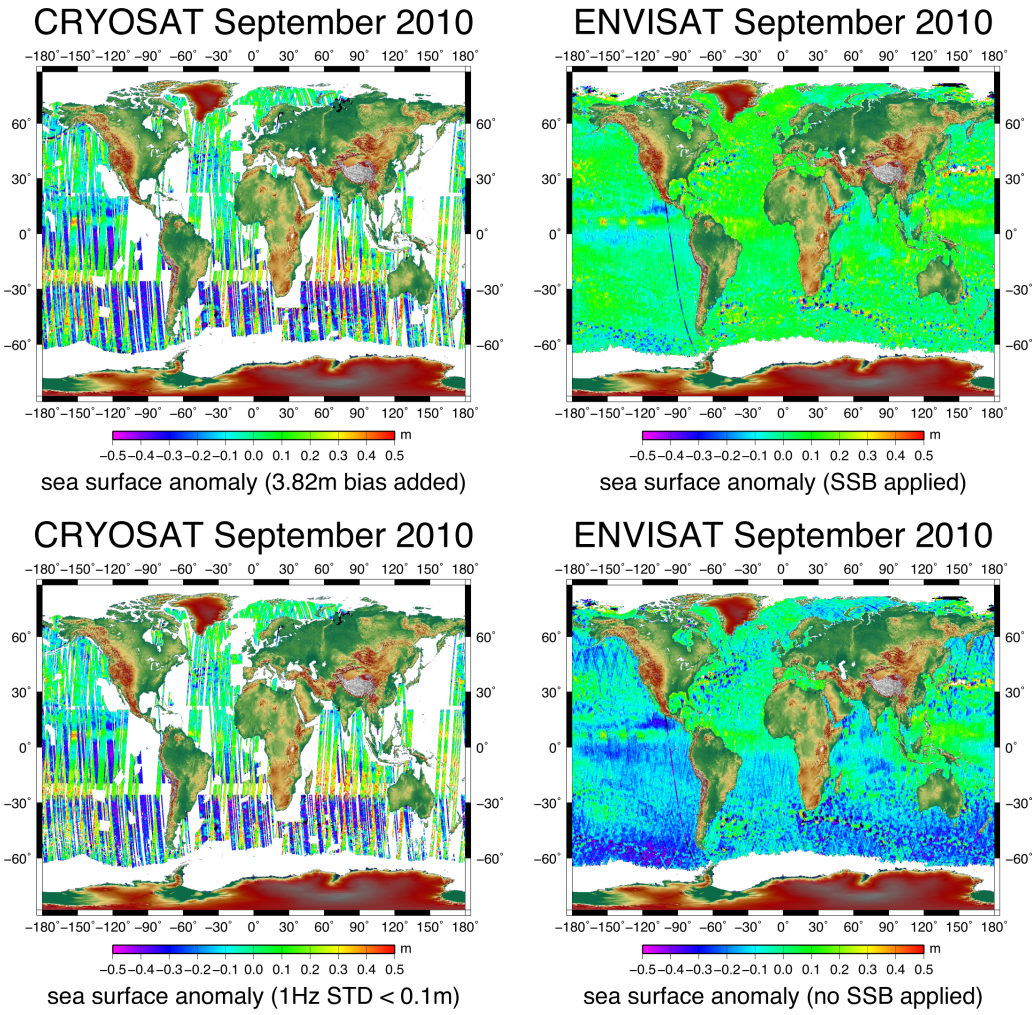

Figure 3.7 Global sea surface anomaly for CryoSat-2 and Envisat with either SSB applied or not. Bottom left: heights only plotted for sea height standard deviation smaller than 10cm

a modest outlier detection. The found mean is -3.82m, and the standard deviation 0.26m, which can be considered fairly noisy. When we do exactly the same with Envisat (plotting the sea surface anomaly w.r.t. to the same reference, in the zonally limited area, covering the same time period, *i.e.* September 2010, and calculating the statistics) we find a mean of 0.04m, and a standard deviation of 0.11m (center panel of Figure 3.6). In other words there seems to be a relative bias between Envisat and CryoSat-2 of -3.86m. Notice that the standard deviation is much less for Envisat. Recalling the fact that de facto we have not applied the sea state bias because it is not available 99% of the time a better comparison is made when also the sea state bias correction is left out for Envisat. The result of that is displayed in the right panel of Figure 3.6: then a mean of -0.1m is found, which translates into a CryoSat-2 range bias of -3.72m. From the difference of the sigma's for Envisat with and without SSB we get a feel for the contribution of the SSB to the "noise" of the data. At the same we have to conclude that only leaving out SSB cannot explain the rather high "noise" in the CryoSat-2 data.

In Figure 3.7 we plot the sea surface anomalies (color-coded) and observe a number of concerns, which basically were already raised. In an (almost perfect) world the top left and right panel should show the same thing, which is anomaly

mainly due to averaged ocean dynamics in September 2010. That we don't live in a perfect world is shown in the Envisat plot where one track appears to have an outlying orbit error. Now in the CryoSat-2 plot we see a lot of data gaps, but these can be easily attributed by the different modes of the SIRAL instrument; we are only looking at the LRM part of the data. The disturbing thing in this plot is the "noise" and average offset of around 30cm in the ascending tracks and mainly in the area below 30°S. According to the experts at ESTEC this is to be attributed to the earlier mentioned problem with the ground processing that takes care of the re-tracking of the waveforms (OCOG vs. CFI). This will be addressed in a new version of the software so we will not look further for explanations. Because of the SSB mishap a more honest comparison is obtained by leaving out the SSB correction from the Envisat anomalies. This is portrayed in the bottom right panel of Figure 3.7. If we then also edit the CryoSat-2 anomalies and reject measurements for which the 1 Hz standard deviation (coming from a 3rd order polynomial fit through the individual 20 Hz measurements) is larger than 10cm (bottom left panel), we can conclude that for those areas that are not affected by the re-tracker problem the comparison turns out very good. For instance in the Gulf Stream region we observe similar sea level anomalies for CryoSat-2 and Envisat, which encourages us to keep on working on the improvement of the CryoSat-2 data, also for ocean applications. CryoSat-2 could become indispensable to improve spatial and temporal resolution of the Jason altimeter satellites when Envisat would stop working in the near future and to bridge the gap with the next generation of ESA altimeter missions like SENTINEL-3. Comparing the Envisat SSB-case with the Envisat No-SSB-case it is also important to conclude that leaving out the effect of SSB means a serious degradation of the ocean product; so this needs proper attention. During the commissioning phase we reported several inconsistencies in the ground processing chain to ESA. This will continue in the operational phase where we will pay special attention to the ionosphere and wet troposphere corrections as there is no direct measurement for these available on CryoSat, that is no dual-frequency altimeter and no radiometer present.

3.5 L2LRM conclusions

All but one corrections for reducing altimeter range measurements to sea surface anomaly have values within expected range and compare well with other satellites.
Major concern for sea state bias (and related significant wave height and wind speed); only present near LRM/SAR transitions. This limits the usefulness of data for ocean applications and the success of crossover analyses for data component comparisons and orbit accuracy assessment.
From global analysis (restricted to $-60°/+60°$ North) follows a bias of -3.82m relative to the CLS01 MSS, and -3.72m relative to Envisat[a] (no SSB applied).
Data gaps explainable with SIRAL mode map, but zonal banding between $-25°$ and $-20°$ introduces discontinuities likely to be caused by the tracker which requires further investigation in the operational phase.

[a] Envisat bias removed w.r.t. TOPEX frame

Chapter *4*

WP 530: Tide Gauge Calibration of SIRAL - Commissioning Phase

This section concerns the activities for the (absolute) tide gauge calibration of the SIRAL LRM Level-2 data and provides the status at the end of the Commissioning Phase. This work, referred to as WP 530 in the "CryoSat-2 Precise Orbit Determination and Indirect Calibration of SIRAL" project plan, entailed preparing logistics for the use of tide gauges in Lake Erie and other parts of the Great Lakes and tide gauges near Hawaii. Subsequently the altimeter data has to be subjected to the direct comparison with tide gauge data to be able to establish both relative bias and absolute bias. Especially the latter could give insight in possible bias drifts which would be obscured by drifts in the TOPEX frame when we would restrict ourselves to cross-calibration with other satellites (all unbiased w.r.t. to the TOPEX frame). The results that are presented here are limited in usefulness because of the data problems mentioned in the previous Chapter. This has been acknowledged by ESA, and adding to this the importance of a continuous monitoring of range bias and time tag bias we will continue the tide gauge calibration activities in the Operational Phase.

4.1 Work package tasks, inputs and outputs

Tasks defined under WP 530:

- Altimeter bias and drift estimate from tide gauges
- Orbit centering and monitoring

For this we have the following inputs:

- Input from WP 430
- Tide gauge data Lake Erie and UHSLC
- DEOS orbits from WP 310, and SSALTO orbits
- Directives from WP 120

And the following output:

- Reports about altimeter drift assessments
- Reports about geographical orbit pattern

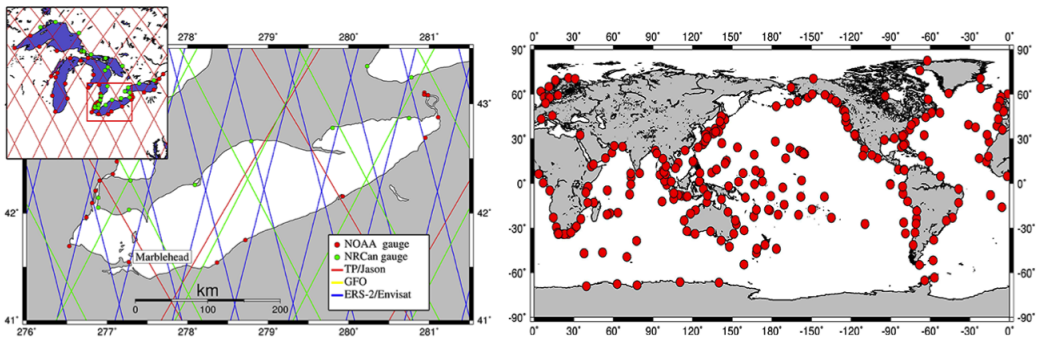

Figure 4.1 Tide gauge locations used for absolute calibration of CryoSat-2 SIRAL LRM Level-2 data (left panel) and tide gauge locations (UHSLC network) used for relative calibration (right panel)

4.2 Tide gauge calibration

The baseline tide gauge calibration methodology established in the readiness report (Development Phase) is defined by the following:

- Conducting verification of SIRAL (along with DEOS and/or CNES precise orbits) over the Lake Erie calibration site, possibly over other parts of the Great Lakes and over oceanic tide gauge sites like near Hawaii.
- Inter-comparing CryoSat-2 with different radar altimetric and laser altimetric (ICESAT, if available) data over the Great Lakes.
- Assessing the (detectability of) CryoSat-2's orbital drift and establishing an error budget.
- Formulating plans for long-term monitoring of the radial orbital drift, reference frame stability, geocenter variations, etc., and providing recommendations for long-term continuous monitoring orbital stability and SIRAL bias drifts and accelerations.
- Solving interpolation issues (from data point to tide gauge location).

Part of the work is carried out by what we call the Ohio group (C.K. Shum and Y. Yi from the School of Earth Sciences at the Ohio State University). This group has a long track record in monitoring lake level changes using satellite altimetry and GPS buoys. Primary objective of these studies is to demonstrate the use of space geodetic measurements (radar altimeters and GPS-buoys) for improving temporal and spatial resolutions of measurements for absolute lake elevation, wave height, wind speed, water vapor and lake ice boundary, and to potentially improve the accuracy in the current operational Great Lakes forecast systems. Data analysis from field campaigns in Lake Michigan demonstrated the use of the GPS-buoy water level instrument for measuring lake water level in any part of the lake and for its use for absolute calibration of altimeters. GPS-buoy campaigns in Lake Erie near the Marblehead water level gauge have been conducted to prepare for the absolute calibrations of new and historic radar altimeters, including GFO, Jason, Envisat, T/P, ERS-2, and now CryoSat-2. Absolute calibration of altimeters is critical for their use to measure global sea level and to conduct climate change studies. Figure 4.1 shows the locations of tide gauges where the (absolute) calibration takes place. Also included are ground tracks of other altimeter satellites. Unfortunately up to now we did not have had any (useful) CryoSat-2 data over Lake Erie and therefore absolute calibration has been postponed. For a number of

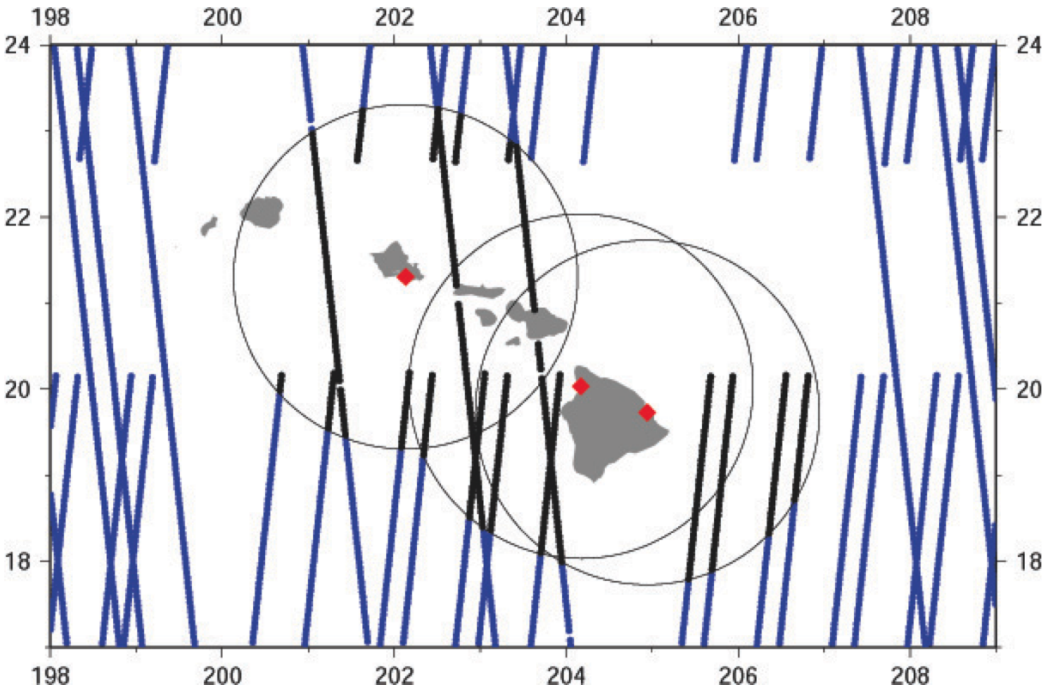

Figure 4.2 Geometry for CryoSat-2 relative tide gauge calibration with 3 tide gauges near Hawaii (indicated with the red diamonds). Also shown are the satellite ground tracks, plotted in black when they enter the "visibility" circle of the tide gauge

these sites we have access to high-frequency sampling and low latency data, and continuous and collocated GPS. Relative calibration uses available data from the global tide gauge network from the University of Hawaii Sea Level Center (UHSLC). A first estimate of relative bias was obtained by adopting three tide gauges near Hawaii. This is discussed in the next section.

4.3 Experiences with relative calibration of SIRAL using tide gauges

Our tide gauge analysis focuses on three NOAA/COOPS (Center for Operational Oceanographic Products and Services) tide gauge stations situated near Hawaii: Honolulu close to Oahu, and Kawaihae and Hilo Bay close to Big Island. Figure 4.2 gives an overview, the read diamonds represent the tide gauges. In this plot also the CryoSat-2 ground tracks have been plotted. We only consider data that is in the vicinity of the tide gauge as indicated by the circles ("horizon" of 400km diameter). Due to the paucity of range data points produced by the CFI ocean re-tracker, those data points have been excluded from the analysis. Instead, only OCOG re-tracker's range data have been used, which are much more abundant although whose height error bit has been flagged during the generation of the Level-2 data product. The problem of this re-tracker choice is the lack of consistent sea state bias (SSB) corrections to the range, and the range itself seems to be uncalibrated (internally). This has been discussed before. Nevertheless we want to perform a relative tide gauge calibration 1) to have a first estimate of bias (which can be compared with what comes from cross-calibration), and 2) to test the software and logistics.

The result is portrayed in Figure 4.3. It shows sea level curves for each of the

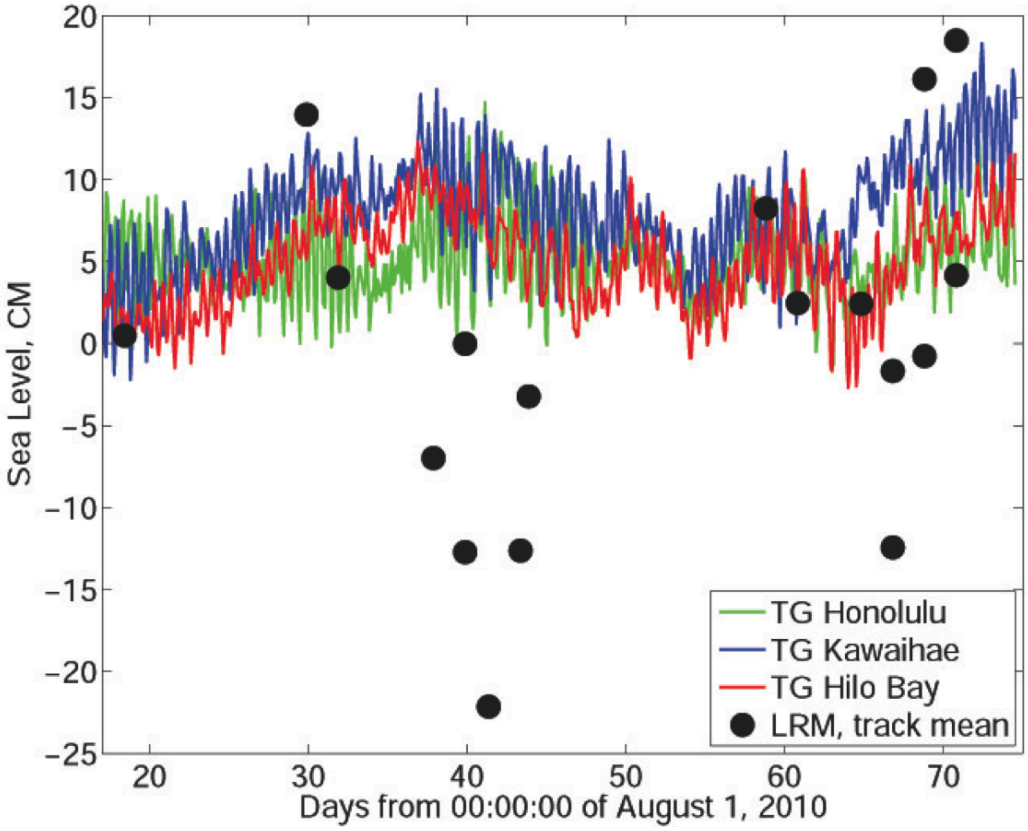

Figure 4.3 Direct comparison of CryoSat-2 compressed sea surface anomaly (black dots) with averaged tide gauge recorded sea level at the tide stations (coloured curves)

three tide gauge sites under investigation. We use compressed 6-minute gauge data w.r.t. a mean sea level (MSL) and de-tide them using the COOPS predicted tide, and average them straightforward to 1 per 2hr data. These are the coloured curves in the figure. The black dots represent the CryoSat altimeter results: they are based on LRM Level-2 corrected height data above CLS01 MSS (in previous sections referred to as sea surface anomaly). An arbitrary bias of 3.8 m. was added to bring the average of the solutions close to zero ("mean sea level"). Remember that a similar value for the range bias was found during cross-calibration with Envisat. Furthermore, we removed the Inverse Barometer correction from the corrected height ("undo" the IB), for a better agreement with the tide gauge data (the DAC correction, though, is retained). Note: all the tide corrections including model ocean tide correction have been applied. Clearly tidal effects in altimetry only cancel after averaging over a very long period due to tidal aliasing. The range correction flags for DAC and sea state bias corrections are ignored because too many 1 Hz corrections are flagged. The altimeter data is subsequently compressed by fitting a line through the 20 Hz data to obtain 1 Hz values (robust fit). Then, the 1 Hz data is averaged within the 3 circles (Figure 4.2) for each track segment to arrive at the black dots in Figure 4.3.

So, in conclusion, the OHIO tide gauge comparison does confirm the bias found by TUDelft, but falls short with the expectations. We notice excursions up to 20cm away from the tide gauge indicated sea level. This has to be attributed to the OCOG re-tracker not being on par with the CFI ocean re-tracker, leading to uncalibrated heights and inconsistent (for 99% of the time missing) SSB. Together

with models for the ionospheric correction and wet troposphere correction we are currently far away from what would be possible for CryoSat: there is a clear need of validation of data **and** corrections in the Operational Phase. Knowing that most data "problems" have been addressed, their origin known, and software revisions underway, we are concerned but not worried about CryoSat's usability in ocean applications. As mentioned in the introduction of this chapter we will continue the tide gauge assisted calibration in CryoSat's Operational Phase.

4.4 Tide gauge calibration conclusions

CFI re-tracked corrected height data cannot be used at the moment, because they are too few. Inferior OCOG re-tracked corrected height measurements are usable but suffer from SSB problems. This has to be addressed in a new round of investigations.
CryoSat-2 comparison with tide gauges near Hawaii reveal the same range bias as found by cross-calibration with Envisat, viz. ≈ 3.8m.
CryoSat-2 comparison with tide gauges near Hawaii fall short with expectations and reveal excursions up to 20cm from the tide gauge sea level. This calls for proper validation and calibration of both data and its corrections in the Operational Phase.
Due to problems with the data, no absolute calibration has been carried out, and also the relative calibration needs revisiting. Here we have to conclude that tide gauge calibration remains important, also in the Operational phase, which we therefore recommend.

Bibliography

ACSL1b (2009), Cryosat ground segment instrument processing facility l1b, (cs-rs-acs-gs–5106), ESA.

ACSL2 (2009), Cryosat ground segment instrument processing facility l2, (cs-rs-acs-gs–5123), ESA.

EADS (2009), Alignment summary document, ESA doc CS-RP-DOR-SY-0055.

ESA (2008), HE-5AS star tracker software interface control document, TER-STR-ICD-001.

Francis, R. (2005), CryoSat reference information, CS-TN-ESA-SY-0441.

Goetz, Christopher (2006), Technical description of the laser retroreflector array cryosat-lrr-02, issue 1.0, c2-dd-raa-lr-0001 (original id: K01-3095-00-00 to), Federal Unitary State Enterprise - Institute for Precision Instrument.

Naeije, M., R. Scharroo, and E. Doornbos (2007), Next generation altimeter service: challenges and achievements, in *Envisat Symposium, Montreux, Switzerland*, ESA SP-636, edited by H. Lacoste, ESA/ESTEC, 23–27 April 2007.

Naeije, Marc, Eelco Doornbos, Lucy Mathers, Remko Scharroo, Ernst Schrama, and Pieter Visser (2002), Radar altimeter database system: exploitation and extension (radsxx), *SRON/NIVR/DEOS publ. NUSP-2 6.3/IS-66 02–06*, Netherlands Agency for Aerospace Programmes (NIVR), Delft, The Netherlands, ISBN 90-5623-077-8.

Naeije, Marc, Remko Scharroo, Eelco Doornbos, and Ernst Schrama (2008), Global altimetry sea-level service: Glass, *NUSP-2 report GO 52320 DEO*, NIVR/DEOS.

Pavlis DE Poulouse S, McCarthy JJ (2006), Geodyn operations manual, contractor report, SGI Inc.

Ries, J (2010), ITRF 2005 SLR coordinates, CSR.

Schrama, E., P.N.A.M. Visser, E.N. Doornbos, M.C. Naeije, B.A.C. Ambrosius, C.K. Shum, and A. Braun (2009), Cryosat-2 precise orbit determination and indirect calibration of SIRAL, proposal submitted to ESA in response to contract change request no. 001 for CCN-2 ESTEC contract no. 18196/04/NL/GS, DEOS.

Willis, P., J.C. Ries, N.P. Zelensky, L. Soudarin, H. Fagard, E.C. Pavlis, and F.G. Lemoine (2009), DPOD2005 : Realization of a DORIS terrestrial reference frame for precise orbit determination, *Advances in Space Research*, pp. 44(5):535–544.